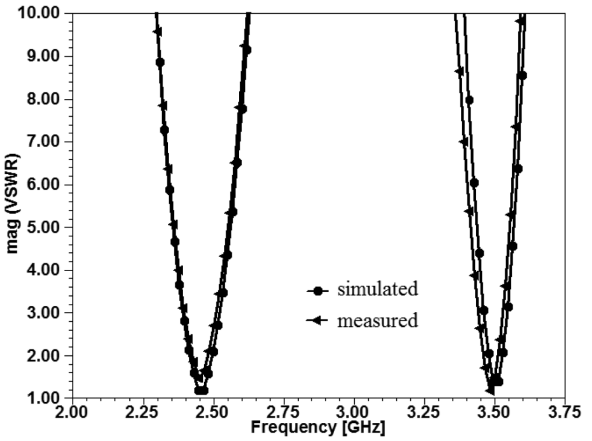

Figure 12 Dual band Behavior of the proposed Antenna 5 in terms of VSWR

ratios of two frequencies f_1 and f_2 obtained in specific range. For variation of spacing S a frequency ratio of 1.28 to 1.47, for variation in width of slots d a frequency ratio of 1.44 to 1.54 and 1.35 to 1.53 for the variation in length of slots L_s is tuned. The proposed antenna with variation in widths w_1 and w_2 a frequency ratio is obtained in the tunable range of 1.40 to 1.45.

The feed point shifted toward right from the centre with a distance d_p to obtain impedance matching, because with increase in L_s, resonance frequency f_2 decreases from 3734 to 3339 MHz, which increases radiation the radiation resistance. The radiation characteristic for Antenna 1 or Reference Antenna and Antenna 5 for lower frequency presented in Figure 10, with broad side directions with minimum cross polarization. A coaxial probe feed is place at a distance d_p from centre for both the modes good impedance matching achieved as shown in Figure 11. From the results of proposed Antenna 5, it has been observed that f_1 is slightly lowered as compared with f_{10} (about 2521 MHz) and f_2 is significantly decreased as compared with f_{30} (about 7618 MHz) in a simple RMSA as shown in Figure 12. The proposed antenna with 2.50 dBi gain and 75% radiation efficiency is noted.

To formalize the prototype is made concerning to the proposed antenna experimentally, the fabrication take place of the modified Antenna 5 and measurement are made using VNA. The antenna is fabricated using FR-4 substrate of height 1.6 mm with 50×54 mm^2 of ground plane. The graph of HFSS simulation and measurement results of fabricated antenna are impersonated in Figure 12 with comparison in terms of VSWR 2:1. Due to margin level in antenna fabrication and connector losses the measured results are departure form HFSS simulation results.

7. CONCLUSION

A simple method using single layer single fed by placing the narrow open ended slots at the edges of simple RMSA accomplish the tunable and dual band operation in this letter slots are placed near the nonradiating edges. Fabrication and measurement of the tunable and dual band RMSA was done through VNA. The measured results and HFSS results are in good agreement. The slots introduced in the structure possess size reduction and compact structure. Bluetooth and WIMAX bands are covered by this antenna in terms of -10 dB $S11$ parameter performance gives impedance matching at two frequencies 2.450–2.4991 GHz and 3.4670–3.5220 GHz with same radiation characteristics. The proposed antenna operates over the tuning frequency ratio in the range 1.41 to 1.45.

REFERENCES

1. S. Maci and G. Biffi Gentili, Dual-frequency patch antennas, IEEE Antennas Propagat Mag, 39 (1997), 13–20.
2. S.T. Fang and K.L. Wong, A dual-frequency equilateral-triangular microstrip antenna with a pair of narrow slots, Microwave Opt Technol Lett 23 (1999), 82–84.
3. R.K. Vishwakarma and R. Kumar, Rectangular notch microstrip antenna for dual-band operation, In: International Conference on Recent Advances in Microwave Theory and Applications, 2008, pp.675–677.
4. D. Sanchez-Hernaindez, G. Passiopoulos, and I.D. Robertson, Single-fed dual band circularly polarised microstrip patch antennas, Eur Microwave Conf 1 (1996), 273–277.
5. A.K. Singh and M.K. Meshram, Slot-loaded shorted rectangular microstrip antenna for dual band operation, In: Asia-pacific Microwave Conference, Bangkok, Thailand, 2007, pp. 1–4.
6. K.P. Ray and A.A. Deshmukh, Multi-band equilateral triangular microstrip antennas, International Conference on Recent Advances in Microwave Theory and Applications, 2008, pp. 705–707.
7. S. Maci, G. Biffi Gentili, P. Piazzesi, and C. Salvador, Dual-band slot-loaded patch antenna, IEEE Proc Microwave Antennas Propag 142 (1995), 225–232.
8. B. Sharma, D. Bharadwaj, K.B. Sharma, V.K. Saxena, J.S. Saini, and D. Bhatnagar, Broadband dual frequency pentagonal microstrip antenna for wireless communication systems, AMTA (2008), 904–906.
9. K.P. Ray, S. Nikhil, and A. Nair, Compact tunable and dual band circular microstrip antenna for GSM and bluetooth applications, Int J Microwave Opt Technol 4 (2009), 205–210.
10. Y. Xiao, D. Su, Y. Wang, and Y. Zhou, Planar compact multiresonator broadband microstrip antenna with slots loading, Antenna Propag EM Theory (2006), 1–3.
11. U. Chakraborty, A. Kundu, S.K. Chowdhury, and A.K. Bhattacharjee, Compact dual-band microstrip antenna for IEEE 802.11a WLAN application, IEEE Antenna Wireless Propag Lett 13 (2014), 407–410.
12. G.-B. Hsieh, M.-H. Chen, and K.-L. Wong, Single fed dual band circularly polarized microstrip antenna, Electron Lett 34 (1998), 1170–1171.
13. G. Kumar, and K.P. Ray, Broadband microstrip antenna, Artech House Publication, Norwood, MA, 2003.
14. [14]Ansoft, High frequency structure simulator, HFSS. v. 13.0, Ansoft, Pittsburgh, PA.

© 2015 Wiley Periodicals, Inc.

CRPA ARRAY WITH RADIATING SLOTS FOR GPS APPLICATIONS

Dae-Heon Lee,[1] Woong-Hee Kim,[1] Dong-Hoon Shin,[1] Jin-Chun Wang,[1] and Hosung Choo[2]
[1] Attached Institute of Electronics and Telecommunications Research Institute, Daejeon, Korea; Corresponding author: leedh@ensec.re.kr
[2] School of Electronic and Electrical Engineering, Hongik University, Seoul, Korea

Received 29 January 2015

ABSTRACT: *This letter proposes the design of a slot-loaded controlled reception pattern antenna) array with ground slot radiators to enhance the radiation gain at low-elevation angles. The array consists of three microstrip patch antennas that are mounted on a circular ground platform, and rectangular slots are inserted at the outer perimeter of the platform. The effectiveness of the inserted slots is verified by comparing the impedance matching and radiating properties of the array with simulation results. The comparison demonstrates that the low-elevation gain of the proposed design can be improved by the slots, which results in a*

broad beamwidth covering most of the upper hemisphere. © 2015 Wiley Periodicals, Inc. Microwave Opt Technol Lett 57:1991–1995, 2015; View this article online at wileyonlinelibrary.com. DOI 10.1002/mop.29230

Key words: *global positioning system antenna; controlled reception pattern antenna array; antenna array; adaptive pattern null*

1. INTRODUCTION

Despite technological advances in global positioning system (GPS) applications, GPS receivers are still vulnerable to interference caused by unwanted in-band signals or intentional jammers. An effective countermeasure against this interference is the use of controlled reception pattern antenna (CRPA) arrays [1] to form adaptive pattern nulls, thereby minimizing the effect of undesired interference while maximizing the power of satellite signals [2–4]. A CRPA array is required to have a wide-beam elevation coverage to receive satellite signals from the upper hemisphere. At the same time, the CRPA must track and generate pattern nulls in the direction of the unwanted interference, which often comes from low-elevation angles in the upper hemisphere [5–7]. Thus, an enhanced gain pattern at a low-elevation angle with a broad beamwidth is a critical aspect of CRPA arrays for improving system performance; however, the pattern distortion of each element, caused by mutual coupling and finite ground plane effects, significantly degrades the adaptive nulling performance and reduces the gain to the satellite direction [8,9]. To mitigate these drawbacks, much effort has been focused on the design of microstrip patch antennas to achieve the required beamwidth for CRPA arrays; however, its intrinsic low-profile characteristic has been obstructive to enhance the gain pattern at low-elevation angles. In addition, most previous studies have concentrated on improving the performance of stand-alone antennas [10,11] without in-depth analysis of CRPA arrays from an adaptive nulling standpoint.

In this letter, we propose a slot-loaded CRPA array to enhance the radiation gain at low-elevation angles with a broad beamwidth using a ground slot radiator. The array is mounted on a circular ground platform, and three ground slots are inserted to improve the low-elevation gain of the individual elements. To verify the effectiveness of the inserted radiating slots, experimental results, such as the return loss, mutual coupling, and radiation patterns, are measured and compared with numerical simulation results. Comparison shows that the proposed design with the radiating slots is suitable to enhance the low-elevation gain with a broadened beamwidth that covers most of the upper hemisphere.

2. ANTENNA CONFIGURATION

Figure 1 shows our design approach and illustrates how the low-elevation gain of an array element can be enhanced using a radiating slot. It is assumed that a microstrip patch antenna is mounted at $\phi = 90°$ with a radius (R_1) of 36.2 mm. A rectangular slot having a length (L_s) of 44.7 mm and a width (W_s) of 2.1 mm is inserted into a circular ground platform at $\phi = 30°$ as shown in Figure 1(a). The antenna pattern at $\theta = 80°$, presented by a dashed line in Figure 1(b), exhibits a significant gain reduction at around $\phi = 30°$. This reduction can be compensated by the resonating slot; thus, the gain of the resulting pattern, expressed by a solid line, can be improved in the direction ($\theta = 80°$, $\phi = 30°$).

Figure 2 shows the configuration of the proposed antenna array, which consists of commercial off-the-shelf ceramic patch antennas (Amotech, model: B25-2D02753-STD70) [12]. The three identical patch antennas are arranged in a uniform circular array with an interelement spacing of about 62.6 mm ($\lambda_0/3$ at

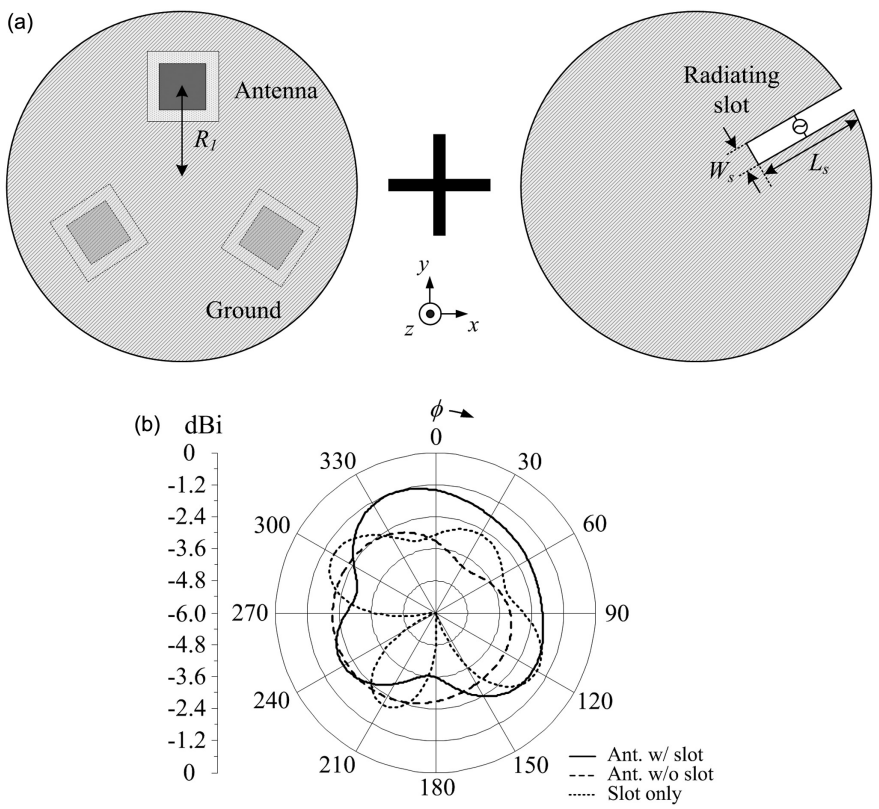

Figure 1 Design approach of GPS antenna arrays with radiating slots. (a) Geometry of radiating slots. (b) Antenna pattern improvement at $\theta = 80°$

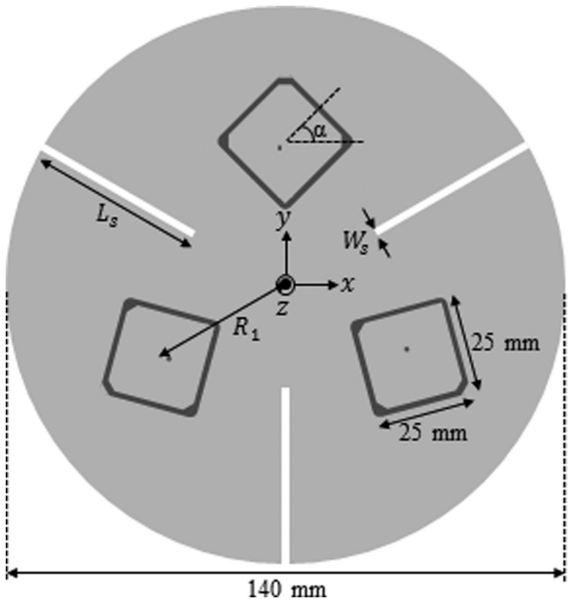

Figure 2 Proposed array configuration

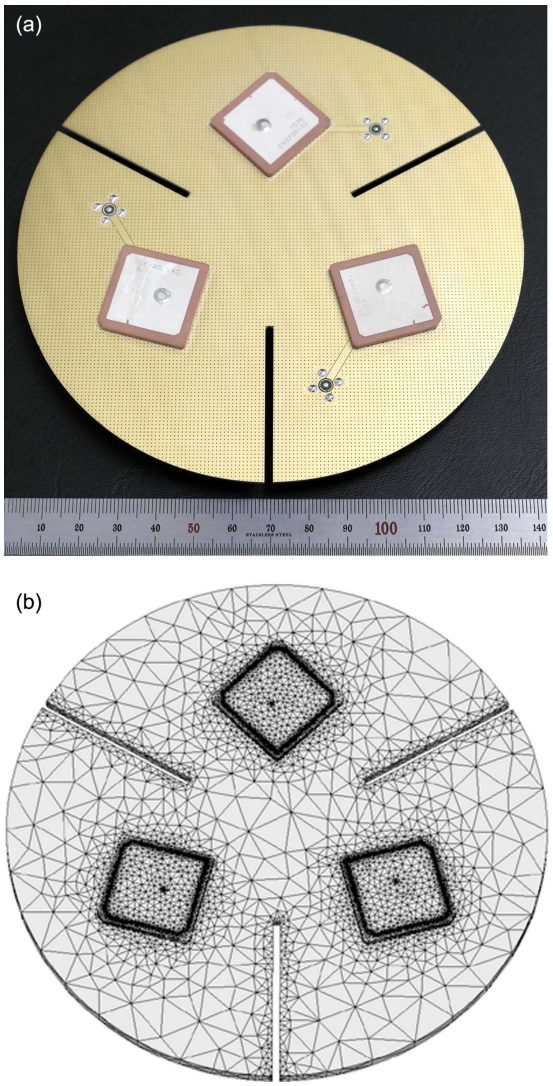

Figure 3 Geometry of the CRPA array. (a) Fabricated antenna. (b) Mesh triangles. [Color figure can be viewed in the online issue, which is available at wileyonlinelibrary.com]

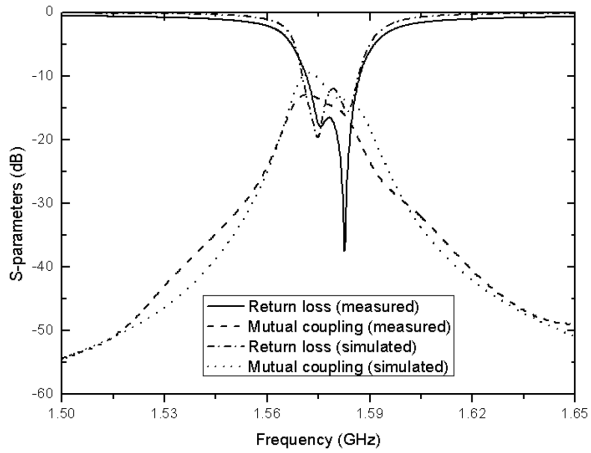

Figure 4 *S*-parameters of the proposed CRPA array

1.57542 GHz) and are mounted on a 5.5-inch circular ground platform. To increase the gain of the individual elements at low-elevation angles, we insert radiating slots in the circular ground platform at an interval of 120°. To make the slot function as a radiator, its length (L_s) is determined to be about a quarter wavelength at 1.57542 GHz. To further improve the beam coverage characteristics, the detailed design parameters of the

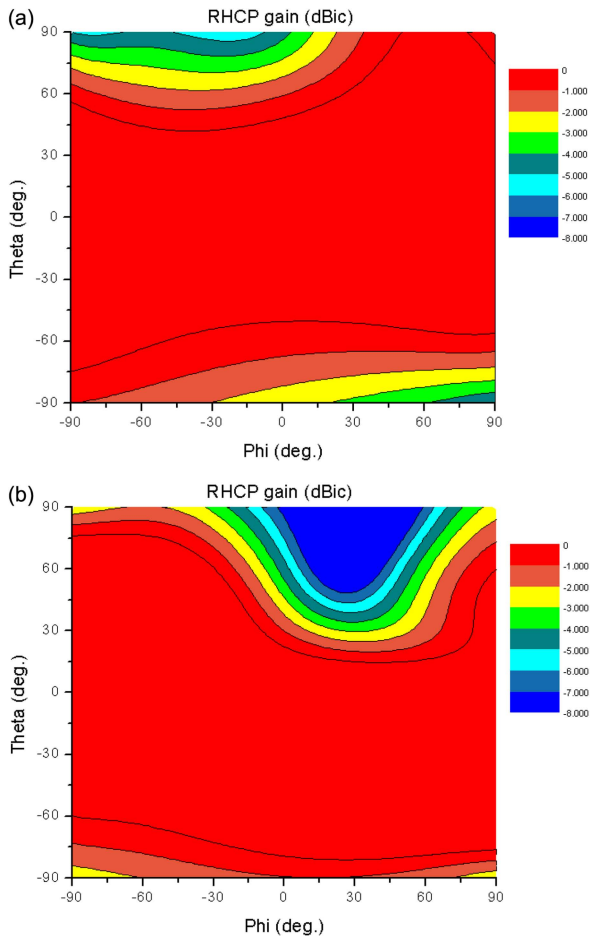

Figure 5 Three-dimensional simulated radiation patterns. (a) Proposed CRPA array (with slot). (b) Reference antenna array (without slot). [Color figure can be viewed in the online issue, which is available at wileyonlinelibrary.com]

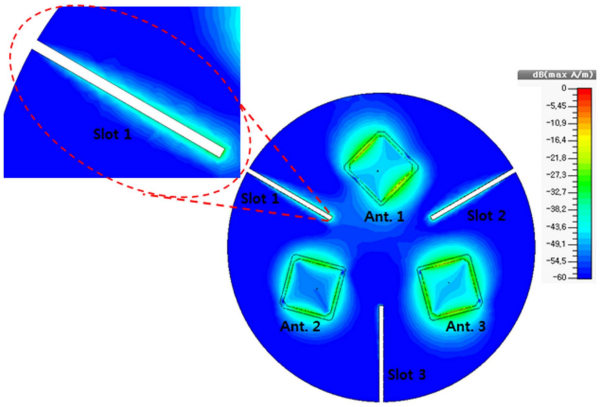

Figure 6 Simulated current distribution of the proposed CRPA array in L1 band. [Color figure can be viewed in the online issue, which is available at wileyonlinelibrary.com]

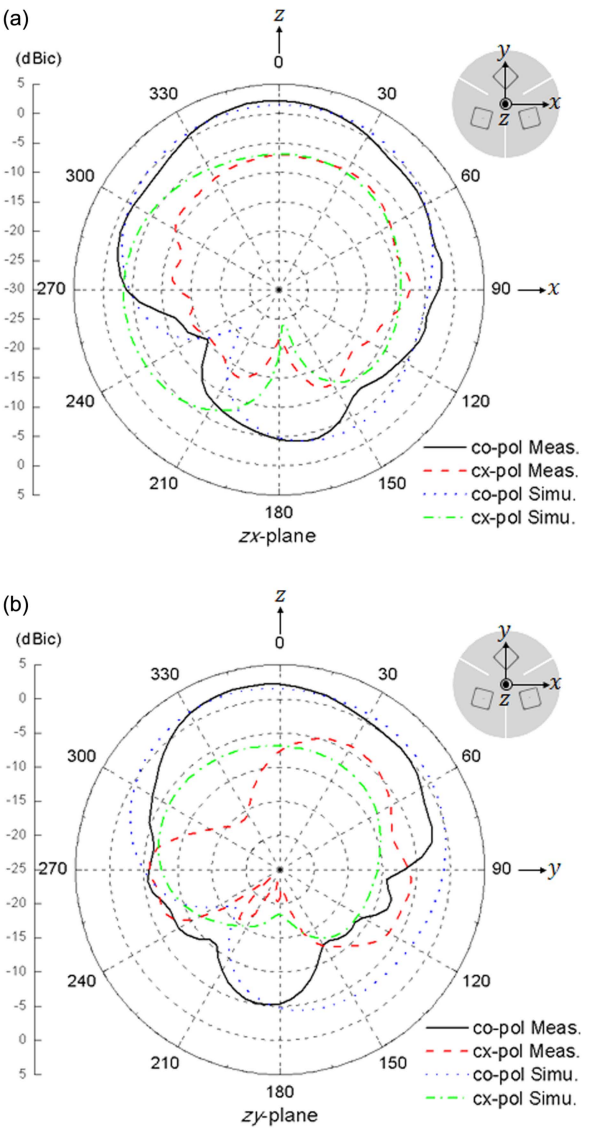

Figure 7 Far-field radiation patterns of the proposed CRPA array. (a) *zx*-plane. (b) *zy*-plane. [Color figure can be viewed in the online issue, which is available at wileyonlinelibrary.com]

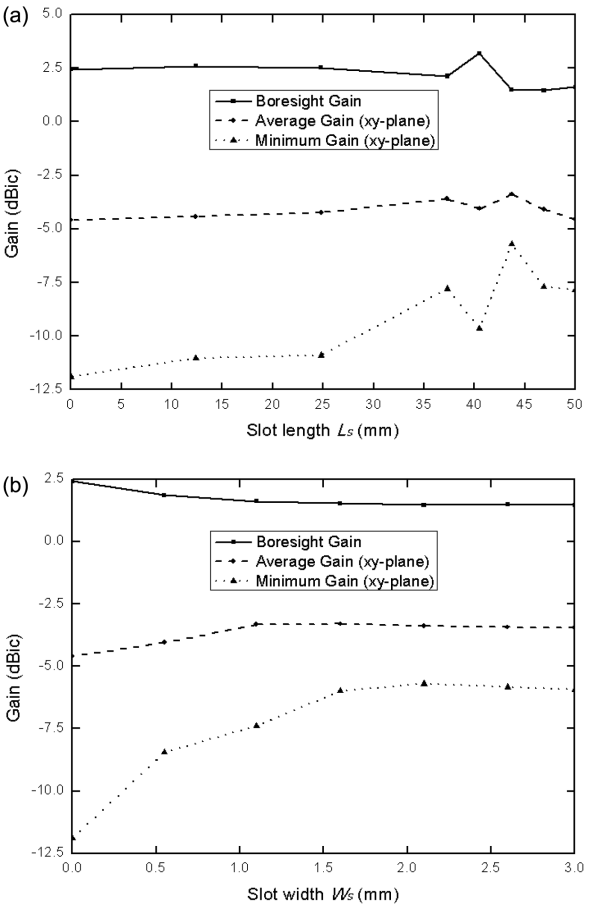

Figure 8 Variations in antenna gains according to slot parameters. (a) Slot length L_s. (b) Slot width W_s

proposed antenna are optimized using the full-wave EM simulation software of Microwave Studio [13]. The optimized parameters are the following: $R_1 = 36.2$ mm, $\alpha = 45°$, $L_s = 43.7$ mm, and $W_s = 2.1$ mm, and photographs of the fabricated antenna and its mesh triangles are shown in Figure 3.

3. RESULTS AND DISCUSSION

The results of the *S*-parameters for the fabricated prototype were measured with an Agilent N5242A vector network analyzer. Figure 4 shows the simulated and measured *S*-parameters for the proposed antenna array. The measured return loss is −17.8 dB in the GPS L1 band, which agrees well with the simulation result. The mutual coupling between elements is less than −15 dB over the frequency band of interest.

To verify the advantage of the proposed ground plane, the antenna gain over the entire upper hemisphere is compared with that of the array without radiating slots, as shown in Figure 5. The right-handed circular polarization (RHCP) gain of the reference antenna is drastically degraded when θ is greater than 60°; however, the proposed antenna array exhibits a minimum RHCP gain of −4.2 dBic at $\theta = 80°$, which shows a 7.6-dB improvement compared with the reference antenna.

Figure 6 shows the simulated current distribution of the proposed antenna array at a frequency of 1.57542 GHz. Antenna element 1 (Ant. 1) is excited, while Ant. 2 and Ant. 3 are terminated with a matched load. The current shown in the dB scale is normalized to the maximum current displayed in the figure. A current density greater than −20 dBA/m is observed around

Slots 1 and 2, which are adjacent to Ant. 1, implying that the slots resonate at this frequency.

Figure 7 shows the plots of the measured far-field radiation patterns compared with the simulation patterns. Figure 7(a) shows patterns in the *zx*-plane at 1.57542 GHz, and its half-power beamwidth (HPBW) is 80°. Figure 7(b) shows patterns in the *zy*-plane at the same frequency with an HPBW of 100°. As can be observed, the antenna satisfies the HPBWs of greater than 80° without any serious gain degradation or pattern distortion, making it suitable for use in CRPA array applications.

We examine the effects of the length L_s and width W_s of the radiating slot (shown in Fig. 2) on the gain characteristics of the proposed antenna. Figure 8(a) shows the simulated antenna gains in relation to the radiating slot length L_s. The average and minimum gains at the *xy*-plane ($\theta = 90°$) are improved as the slot length L_s increases up to $L_s = 47.3$ mm (about $0.23\lambda_0$ at L1 band), which is the optimum slot length in terms of antenna gain. Figure 8(b) shows the simulated antenna gains in relation to the radiating slot width W_s. Although the parameter W_s is less susceptible to the low-elevation gain compared with L_s, its optimum value is observed at $L_s = 2.1$ mm.

4. CONCLUSION

A slot-loaded CRPA array for GPS applications was proposed in this letter. To achieve a wide-beam elevation coverage at the CRPA, radiating slots are inserted into the ground platform. As a result, the proposed antenna array consistently maintains higher RHCP gain over the entire upper hemisphere. In addition, the proposed array with radiating slots has a simple configuration, suggesting the feasibility of a low-cost commercial implementation. From the above results, we concluded that the proposed antenna is suitable for use in GPS CRPA applications without significant pattern distortions or gain degradation.

ACKNOWLEDGMENTS

This research was supported by the Ministry of Science, ICT and Future Planning (MSIP), Korea, under the R&D program supervised by the MSIP.

REFERENCES

1. Z. Fu, A. Hornbostel, J. Hammersfahr, and A. Konovaltsev, Suppression of multipath and jamming signals by digital beamforming for GPS/Galileo applications, GPS Solut 6 (2003), 257–264.
2. I.J. Gupta, T.H. Lee, K.A. Griffith, C.D. Slick, C.J. Reddy, M.C. Bailey, and D. DeCarlo, Non-planar adaptive antenna arrays for GPS receivers, IEEE Antennas Propag Mag 52 (2010), 35–51.
3. Y.H. Chen, A study of geometry and commercial off-the shelf (COTS) antennas for controlled reception pattern antenna (CRPA) arrays, In: Proceedings of the 25th International Technical Meeting of the Satellite Division of ION (2012), Nashville, TN, 2012, pp. 907–914.
4. G. Byun, S. Kim, and H. Choo, Design of a dual-band GPS antenna using a coupled feeding structure for high isolation in a small array, Microwave Opt Technol Lett 56 (2014), 359–361.
5. J.A. Kasemodel, C.C. Chen, I.J. Gupta, and J.L. Volakis, Miniature continuous coverage antenna array for GNSS receivers, IEEE Antennas Wireless Propag Lett 7 (2008), 592–595.
6. J.R. Lambert, C.A. Balanis, and D. DeCarlo, Spherical cap adaptive antennas for GPS, IEEE Trans Antennas Propag 57 (2009), 406–413.
7. M. Chen and C.C. Chen, A compact dual-band GPS antenna design, IEEE Antennas Wireless Propag Lett 12 (2013), 245–248.
8. K.A. Griffith and I.J. Gupta, Effect of mutual coupling on the performance of GPS AJ antennas, In: IEEE/ION Position, Location and Navigation Symposium, Monterey, CA, 2008, pp. 871–877.
9. J. Huang, The finite ground plane effect on the microstrip antenna radiation patterns, IEEE Trans Antennas Propag 31 (1983), 649–653.
10. J. Jan and K. Wong, A dual band circularly polarized stacked elliptic microstrip antenna, Microwave Opt Technol Lett 24 (2000), 354–357.
11. K.P. Yang and K.L. Wong, Dual-band circularly-polarized square microstrip antenna, IEEE Trans Antennas Propag 49 (2001), 377–382.
12. Model B25-2D02753-STD70, Amotech, Available at: http://www.amotech.co.kr, 2012.
13. Microwave Studio, Computer Simulation Technology, Wellesley Hills, MA, Available at: http://www.cst.com, 2014.

© 2015 Wiley Periodicals, Inc.

COMMENT ON "LINEARIZATION OF POWER AMPLIFIERS BY SECOND HARMONICS AND FOURTH-ORDER NONLINEAR SIGNALS" BY A. ATANASKOVIC, N. MALES-ILIC, AND B. MILOVANOVIC

B. R. Dimitrijevic
Faculty of Electrical Engineering, University of Nis, Nis, Serbia;
Corresponding author: bojan.dimitrijevic@elfak.ni.ac.rs

Received 22 December 2014

ABSTRACT: •••. © 2015 Wiley Periodicals, Inc. Microwave Opt Technol Lett 57:1995–1996, 2015; View this article online at wileyonlinelibrary.com. DOI 10.1002/mop.29244

The great majority of the results presented in [1] are essentially reformulated results from previously published papers [2] and [3]. Besides, papers [2] and [3] are not cited in [1], and paper [3] is not cited in the newer paper [2]. This points to the apparent intention of the authors to reuse the same results, concealing important facts from the reviewers in newer paper [2] and finally in [1].

Parts of the paper [1] that are re-used from the previous papers are:

a. Figure 2 from [1] is the same as Figure 4 in [2] and Figure 3 in [3]
b. Figure 6 from [1] is the same as Figure 2 in [2] and Figure 2 in [3]
c. Figure 5 from [1] is mostly the same as Figure 1 in [2] (Figure 1 in [2] has an optional attenuator because of the asymmetry) and completely the same as Figure 1 in [3]
d. Figure 7 from [1] is the same as Figure 7b in [2]
e. Figure 8 from [1] is the same as Figure 8b in [2]
f. Figure 9 from [1] is the same as Figure 9 in [2] and Figure 8 in [3]

The similarities (a) and (b), showing the photos of the implemented modules, indicate that all three papers consider the same hardware implementation.

The similarities (c) indicate that all papers use the same method with the identical configuration.

The similarities (d), (e), and (f) show the same experimental results.

Finally, we can say that the vast majority of the paper [1] is the re-use of the previously published results without citing the